

Research Article

An Automated Multimodal Spectral Cluster Based Segmentation for Tumor and Lesion Detection in Pet Images

¹M. Manoj and ²L. Padmaresh

¹School of Electrical Sciences,

²Department of Electrical Engineering, Noorul Islam University, Kumaracoil, Tamil Nadu, India

Abstract: The acquisition of Positron Emission Tomography (PET) images for tumor and lesion detection has emerged as one of the most powerful tools for medical image analysis in recent years. Works on patch-based sparse representation selected the most relevant elements from a large group of candidates using segmentation, but failed to separate myelinated WM from unmyelinated WM compromising multi-modality image information. In this study, a novel technique to obtain multimodality aspect of tumor and lesion detection in PET images through Automated Multimodal Spectral Cluster based Segmentation (AMSCS) is proposed, aiming at improving the tumor detection accuracy. The Spectral Contours with Constrained Threshold (SCCT) technique in AMSCS is carried out to various spectral features of the PET image without any deformation, improving the true positive rate. The SCCT technique utilize user defined seed point in the region of interest in PET images and generate spectral contours (i.e.,) shape, size, location and intensity. A Multi-Spectral Contour Cluster (MSCC) mechanism is introduced that organizes the spectral contour features of shape, size, location and intensity into multi-spectral clusters for quicker segmentation of PET Image regions of interest. Experimental analysis is conducted using Primary Tumor Data Set from UCI repository PET Images on parametric such as, Multi-spectral cluster size, ROI segmentation time, tumor and lesion detection time, tumor detection accuracy.

Keywords: Constrained threshold, multimodality, positron emission tomography, region of interest, spectral contours

INTRODUCTION

Medical image analysis has witnessed a large scale deployment in a wide range of medical and biological image analysis. Among the available Medical image analysis, multimodality aspect of tumor and lesion detection in PET images is one of the most promising and widely adopted methods. Level Set for Bladder Wall Segmentation (LS-BWS) using a LS function improving the detection ratio in inner and outer borders (Duan *et al.*, 2010). Patch-driven Level Set for Brain Neonatal Segmentation (PLS-BNS) (Wang *et al.*, 2014) performed efficient segmentation on neonatal brain MR images aiming at improving the segmentation accuracy rate, however compromising multi-modality image information, which remains the objective of our mechanism.

In recent years, large amount of research works are conducted on improving the accuracy of features being detected. Detection of renal lesions concentrated in Liu *et al.* (2015) where multi-scale features were used to improve the detection accuracy by also reducing false positives. By applying Independent Component

Analysis (ICA) (Zhao *et al.*, 2014), early detection of down-syndrome was made possible improving the accuracy and F-1 score, compromising automated detection. Automated segmentation (Liu *et al.*, 2014) was performed on ovarian cancer that used an approach called, Tumor Sensitive Matching Flow (TSMF) to improve the detection accuracy. However, the approaches presented above pose significant challenge by compromising the detection time, which the proposed work focus by introducing Multi-Spectral Contour Cluster mechanism. Statistical shaping approach (Mendoza *et al.*, 2014) was used to increase the sensitivity and specificity from CT images. Another approach called Naive Bayes (Huang *et al.*, 2014) was applied for efficient diagnosis of cancer improving the classification accuracy.

Automatic detection and segmentation of dermoscopy images was presented in Madooei *et al.* (2013) improving the detection rate. However, computerized automatic phenomenon was not carried out compromising the detection time. Three way classifications for streaks (Sadeghi *et al.*, 2013) in dermoscopic images were designed improving the

classification accuracy. However, with the increase in scalability, many streaks fitting multiple ellipses were not addressed. Gaussian Mixture and Markov Random model (Layer *et al.*, 2015) for different lesion shapes were used both for small and larger volumes. However, segmentation time for different lesion shapes was not concentrated.

In particular, (1) we present an in-depth analysis on various spectral contours such as shape, location, intensity and size using spectral contours with constrained threshold (2) design of Multi-Spectral Contour Cluster to reduce the tumor and lesion detection time and (3) a novel algorithm is presented integrating segmentation with multi-spectral contour cluster to improve the performance of the segmentation time. Following are the main contributions of this study:

- To obtain multimodality aspect of tumor and lesion detection in PET images through Automated Multimodal Spectral Cluster based Segmentation (AMSCS)
- To improve tumor detection accuracy by designing Spectral Contours with Constrained Threshold
- To minimize the tumor detection time by constructing Multi-Spectral Contour Cluster by evaluating the anchor points, curvature and local regions of tumor and lesions in the PET images.

MATERIALS AND METHODS

Figure 1 shows the proposed technique of Automated Multimodal Spectral Cluster based Segmentation consists of three main steps as summarized Details are presented in the following sections, i.e., construction of Spectral Contours with Constrained Threshold (SCCT) technique from the template images, enforcing Multi-Spectral Contour Cluster (MSCC) mechanism for organizing spectral contour features of shape, size, location and intensity into multi-spectral clusters for quicker segmentation of PET Image and further integrating it into a coupled level set framework for tumor and lesion detection.

Figure 1 shows the block diagram representation of MSCC mechanism is split into three parts. The first part, spectral contours with constrained threshold uses shape, location, intensity and size as spectral contours, aimed at improving tumor detection accuracy and true positive rate.

As shown in Fig. 1, the block diagram of MSCC. The block diagram of MSCC mechanism is split into three parts. The first part, spectral contours with constrained threshold uses shape, location, intensity and size as spectral contours, aimed at improving tumor detection accuracy and true positive rate. The second part, multi-spectral contour cluster measured anchor points, curvature and local regions for similarity using

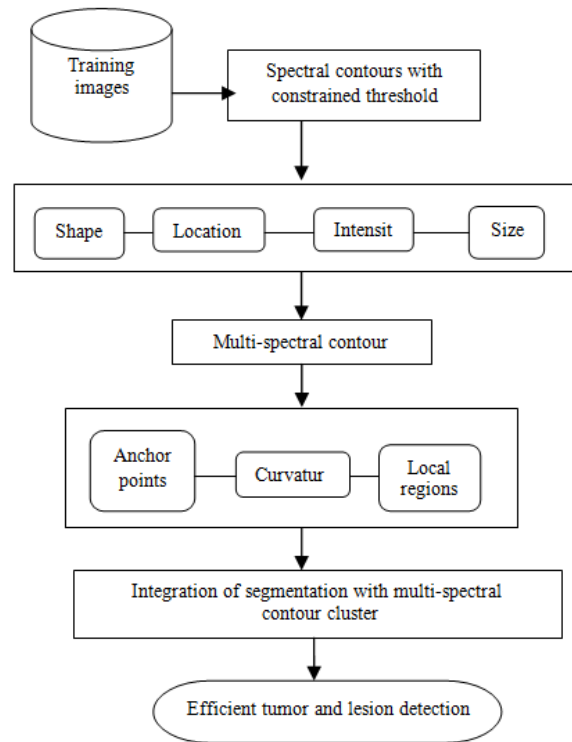


Fig. 1: Block diagram of MSCC mechanism

eigenvector, with the objective of improving location of tumor and lesion being detected. Finally, the third part, integrates segmentation (i.e., identification of global regions of similarity for tumor and lesion detection) with Multi-Spectral Contour Cluster reduces the ROI segmentation time. The elaborate description of each part is provided in the forthcoming sections.

Spectral Contours with Constrained Threshold (SCCT) technique:

The first step involved in the design of Automated Multimodal Spectral Cluster based Segmentation is the construction of Spectral Contours with Constrained Threshold (SCCT) technique. One of the pre-requisites for tumor or lesion diagnosis in PET images is the identification of certain spectral contours where the proposed MSCC mechanism used shape, size, location and intensity for tumor and lesion detection in PET images. The Spectral Contours with Constrained Threshold (SCCT) technique is carried out with several spectral features of the PET image without any deformation. Spectral feature selection aims to select features and reduce the deformation that best optimize the criterion related to the class labels of the data, aiming at reducing the deformation.

To start with, the SCCT technique generates the spectral contour, shape which is approximated by an ellipse model. Let us consider a feature vector ' V ' with five elliptic parameters characterized by location of the center point ' p, q ', Major Region of Interest ' $Major_{ROI}$ '

and Minor Region of Interest ‘ $Minor_{ROI}$ ’ at an angle ‘ \emptyset ’ and is given as below:

$$V = (p, q, Major_{ROI}, Minor_{ROI}, \emptyset) \quad (1)$$

To calculate the similarity for spectral contours with shape as a contour, the proposed framework uses the subspace method. Therefore, the subspace method for obtaining the spectral contour with respect to shape for tumor and lesion detection is used as a region of interest in the proposed mechanism. The similarity is defined by the angle between the subspace ‘ S ’ and the input vector ‘ V ’. The square cosine for shape spectral contour for extracting the shape with constrained threshold is defined as given below:

$$Cos^2 = \frac{1}{V} \sum_{i=1}^n ((V, \emptyset_i)^2) \quad (2)$$

From (2), the square cosine for spectral contour shape, ‘ Cos^2 ’ is equal to the product of ‘ \emptyset_i ’ that represents the bases for the subspace ‘ S ’ for ‘ n ’ dimensional subspace. Once the shape is defined, the SCCT technique defines a function $fn(a, b, \emptyset)$ that significantly predicts the probability of a spectral feature with location ‘ \emptyset ’ at each image pixel (a, b) .

Let us consider an image ‘ $Image_i$ ’, then the construction of functional contour detection that predicts the probability of a spectral feature is the evaluation of a seed point signal ‘ $SP(a, b, \emptyset)$ ’. This computation proceeds by placing an ellipse at location ‘ (a, b) ’ that is divided into two portions at an angle ‘ \emptyset ’. The functional contour detection with seed point signal, ‘ SP ’ at location ‘ (a, b) ’ is then defined as given below:

$$SP^2(a, b) = \frac{1}{2} * \frac{(a(i) - b(i)^2)}{a(i) + b(i)} \quad (3)$$

Based on the location (i.e., seed point signal) obtained from (3), the functional contour detector integrates the user defined seed point signals obtained from transforming an input image into four distinct spectral features stored in a vector as Vector Intensity ‘ VI ’ and is formulated as given below:

$$VI = (Image_i, LI, HI, UI) \quad (4)$$

where $LI = (0 - 128), HI = (128 - 255), UI = (64 - 92)$

From (4), by processing each feature independently, the last three corresponding spectral features stored in the vector refer to the corresponding intensity, to as Low Intensity ‘ $LI (0-128)$ ’, High Intensity ‘ $HI (128-255)$ ’ or Uniform Intensity ‘ $UI (64-192)$ ’. In order to detect the size, the difference between two regions (i.e., major region of interest and minor region of interest) is obtained on the basis of linear

pattern. The spectral contour size is formulated as given below:

$$Size = \frac{(Minor_{ROI} - Major_{ROI})^2}{T^2} \quad (5)$$

$$(Minor_{ROI})^2 = i1 (LI - HI)^2 + i2 (UI - HI)^2 \quad (6)$$

$$T^2 = \sum (LI * HI)^2 \quad (7)$$

where ‘ LI, HI and ‘ UI ’ is the image pixel intensity. The above user defined seed point in the region of interest in PET images is utilized for various spectral features of the PET image. Once, the spectral contours features of shape, size, location and intensity are organized, multi-spectral clusters are performed for quicker segmentation which is detailed in the forthcoming sections.

Multi-Spectral Contour Cluster (MSCC)

mechanism: The second step involved in the design of Automated Multimodal Spectral Cluster based Segmentation is the construction of Multi-Spectral Contour Cluster (MSCC) mechanism. The MSCC mechanism organizes the spectral contour features of shape, size, location and intensity into multi-spectral clusters, aiming at reducing the time taken to locate the tumor and lesion being detected. This is obtained by evaluating the anchor points, curvature and local regions of tumor and lesions in the PET images.

To start with, let us define the multi-spectral clustering problem. Given a set of input patterns ‘ $Patterns_i$ ’, using multi-spectral feature vectors ‘ V ’, that is given as below:

$$FV = (F_1, F_2, \dots, F_n) \quad (8)$$

where, (8), ‘ F_1, F_2, \dots, F_n ’ represent the multi-spectral features and these features are grouped with features. An affinity matrix ‘ $A = (A_{ij})$ ’ is formed on the assumption that the elements in A_{ij} measures the similarity between the ‘ i th’ and ‘ j th’ multi-spectral feature vectors. However, to improve the location of tumor and lesion being detected, the proposed AMSCS technique uses eigenvector for efficient clustering which is formulated as given below:

$$W_i = \lambda(A_{i,1}V_1 + A_{i,2}V_2 + \dots + A_{i,n}V_n) \quad (9)$$

$$= \sum_{j=1}^n A_{ij}V_j \quad (10)$$

From (9) and (10), ‘ V ’ is the eigenvector of the linear transformation A and the scale factor λ is the anchor point corresponding to that eigenvector for tumor and lesion detection in PET images. Based on the eigenvector values, which has the pixel difference

between two clusters ‘ A_i ’ and ‘ A_j ’, the two clusters are combined to form ‘ A_{ij} ’ and the new centroid pixel value is evaluated and is given as below:

$$C_{ij} = \frac{A_i + A_j}{2} \quad (11)$$

where, ‘ C_{ij} ’ represents the centroid value and is obtained by the average of the two clusters ‘ A_i ’ and ‘ A_j ’ respectively. Let us assume that the local similarities (i.e., local regions) are more reliable (i.e., perform quicker segmentation) than the far-away regions (i.e., global regions). With this assumption, the unreliable neighbors (i.e., regions) are removed. To remove the unreliable neighbors (i.e., regions of interest), the proposed AMSCS technique uses the k nearest neighbor’s technique in order to identify the associated similarity affinity matrix ‘ A ’:

$$A'_{i,j} = A_{i,j} \text{ where } Image_i \in KNN(Image_j), \\ Image_j \in KNN(Image_i) \quad (12)$$

where, ‘ KNN ’ denotes the K Nearest Neighbors of multi-spectral features of image ‘ $Image_j$ ’ and ‘ $A_{i,j}$ ’ and ‘ $A'_{i,j}$ ’ denotes the affinity matrix and new affinity matrix obtained through K Nearest Neighbors.

The above steps followed through KNN in MSCC result in the formation of new cluster ‘ $A_{i,j}$ ’ from the two individual clusters ‘ A_i ’ and ‘ A_j ’ with the greatest similarity. As a result, with the proposed MSCC mechanism, the total number of clusters is reduced by one after the other after successive iteration, improving location of tumor and lesion being detected.

Integration of segmentation with multi-spectral contour cluster: The final step involved in the design of Automated Multimodal Spectral Cluster based Segmentation is the effective integration of Segmentation using Multi-Spectral Contour Cluster into a coupled level set framework for tumor and lesion detection in PET images. The integration is provided using Segmentation with Multi-Spectral Contour Cluster (SMSCC) algorithm.

The SMSCC algorithm provides an efficient means to obtain multimodality aspect of tumor and lesion detection in PET images. The algorithm is divided into three parts. The first part utilized user defined seed point in the region of interest in PET images by generating the spectral contours (i.e.,) shape, size, location and intensity. A subspace method for extracting ellipse as a shape contour using major and minor region of interest was used for each PET images. Then, by applying the seed point signal, the location analysis with constrained threshold was used with vector intensity derived between 0 and 255.

Finally, with the integration of segmentation and multi-spectral clustering using global measures for obtaining the regions of similarity, the anchor points attract the contour toward the boundary of PET images resulting reducing the segmentation time.

RESULTS AND DISCUSSION

This section describes the process of evaluating the AMSCS mechanism to obtain multimodality aspect of tumor and lesion detection in PET images. The AMSCS mechanism is evaluated in different aspects, multi-spectral cluster size, ROI segmentation time, location of tumor and lesion, tumor detection accuracy, using training images extracted from Primary Tumor Data Set from UCI repository. The AMSCS mechanism is implemented using MATLAB to enhance the location of tumor and lesion being detected at a faster rate with minimal ROI segmentation time and therefore improve the tumor detection accuracy. AMSCS mechanism is compared on the existing Level Set for Bladder Wall Segmentation Duan *et al.* (2010) and Wang *et al.* (2014) and compared to Patch-driven Level Set for Brain Neonatal Segmentation PLS-BNS.

Measure of tumor detection accuracy: Tumor detection accuracy measures the accurate detection of tumor and lesion in patients. It is the ratio of number of images (i.e., patients) correctly detected to be of tumor to the total number of images provided as input (i.e., total number of patients). The tumor detection accuracy is measured in terms of percentage (%):

$$A = \frac{\text{No of images}_{CD}}{\text{Image}_n} * 100 \quad (13)$$

From (13) ‘ CD ’ refers to the correctly detected lesions where ‘ n ’ number of images provided as input. This is because with the application of Spectral Contours with Constrained Threshold (SCCT) technique, the AMSCS mechanism based on feature selection reduces the deformation that best optimize the criterion related to class labels of the data and therefore increasing the tumor detection accuracy by 16.48 % when compared to Duan *et al.* (2010), LS-BWS method.

Furthermore, by applying the subspace method various spectral features of the PET image is processed without any deformation with user defined seed point that significantly predicts the probability of a spectral feature, improving the tumor detection accuracy by 31.61% Wang *et al.* (2014), compared to PLS-BNS respectively (Fig. 2).

Measure of tumor and lesion detection time: Tumor and lesion detection measures the proportion of actual

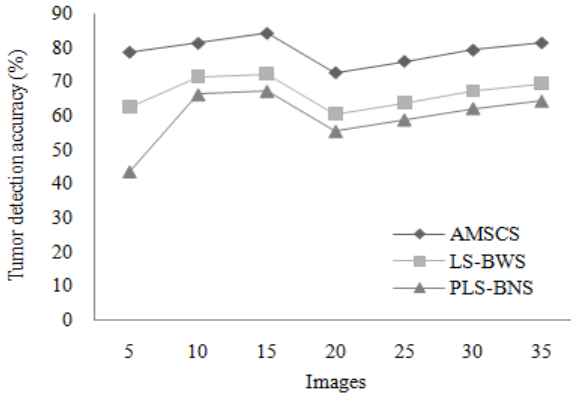


Fig. 2: Measure of tumor detection accuracy with respect to 35 images

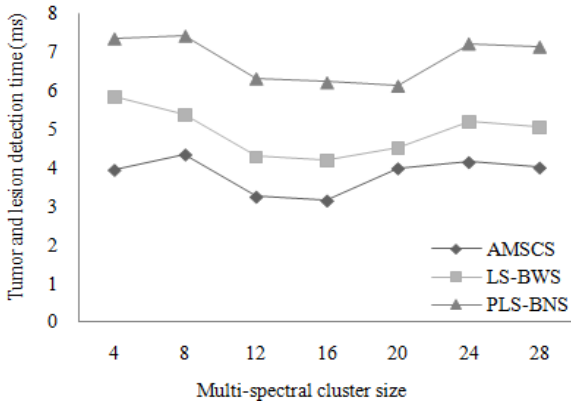


Fig. 3: Measure of tumor and lesion detection time

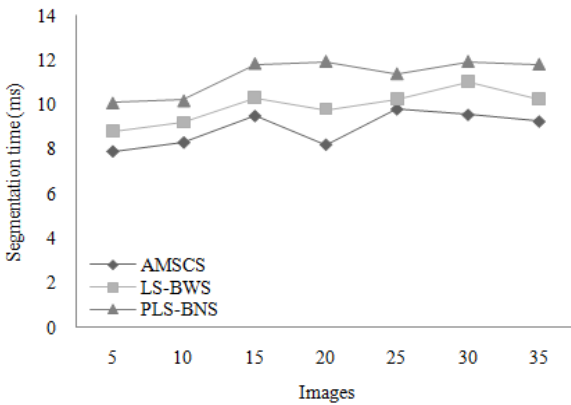


Fig. 4: Measure of segmentation time with respect to images

detection of tumor which is correctly identified as such (e.g., the percentage of actual detection of tumor who is correctly identified as having the condition). It is measured in terms of milliseconds (ms) and lower the tumor and lesion detection time more efficient the method is said to be:

$$TLD_{time} = Time (shape + size + location + intensity) \quad (14)$$

From the Fig. 3, the time for detecting tumor and lesion using the proposed AMSCS mechanism is lower when compared to two other existing works (Duan *et al.*, 2010), LS-BWS and PLS-BNS (Wang *et al.*, 2014) respectively. Comparatively, it is observed to be lower using the proposed mechanism, AMSCS because of the effective application of Multi-Spectral Contour Cluster that organizes the spectral contour features of shape, size, location and intensity by evaluating the anchor points, curvature and local regions of tumor and lesions in the PET images.

With the identified anchor points, curvature and local regions of tumor and lesions, the tumor and lesion detection time is Duan *et al.* (2010), reduced by 30.81% than LS-BWS. In addition, with the application of the multi-spectral feature vectors that efficiently removes the unreliable neighbors and therefore reducing the tumor and lesion detection time (Wang *et al.*, 2014) by 75.54% than compared to the PLS-BNS respectively.

Measure of segmentation time: Segmentation time refers to the time taken to segment for tumor and lesion detection to the number of images given as input and it is measured in terms of milliseconds (ms):

$$Time = \frac{Time (MajorROI) + Time (MinorROI)}{Image_n} \quad (15)$$

From (15), the segmentation time measures the time taken to obtain major ROI and minor ROI. Lower the segmentation time, more efficient the method is said to be:

Our approach differs from the Duan *et al.* (2010), LS-BWS and PLS-BNS in Wang *et al.* (2014) that we have incorporated the Segmentation using Multi-Spectral Contour Cluster into a coupled level set framework for tumor and lesion detection in PET images that improves the segmentation time by 12.05% compared to Duan *et al.* (2010), LS-BWS and 31.04% compared to Wang *et al.* (2014) PLS-BNS respectively. This is represented in Fig. 4. By applying global measures for obtaining the regions of similarity, anchor points attract the contour toward the boundary of PET images.

CONCLUSION

Medical image analysis for tumor and lesion detection has become the key for PET images to improve tumor detection accuracy and minimize the tumor and lesion detection time at an early stage. In this study, we investigate the performance effects of multimodality aspect of tumor and lesion detection in PET images to categorize the tumor and lesion being detected at an early stage and propose a mechanism called Automated Multimodal Spectral Cluster based Segmentation (AMSCS). The AMSCS mechanism is based on the multi-modality image information that minimizes the effects of multi-modality image

information and greatly improves the detection efficiency. First, the study of Spectral Contours with Constrained Threshold is made that utilize user defined seed point in the region of interest in PET images and generate spectral contours (i.e.) shape, size, location and intensity, aiming at improving the tumor and lesion detection accuracy. Second, a Multi-Spectral Contour Cluster (MSCC) mechanism is developed that effectively organizes spectral contour features of shape, size, location and intensity into multi-spectral clusters for performing quicker segmentation with PET images. Finally, the work integrate Segmentation with Multi-Spectral Contour Cluster using anchor points, curvature and local regions to reduce the time taken for segmenting tumor and lesion using Primary Tumor Data Set from UCI repository. The experiment conducted using Primary Tumor Data Set shows that the AMSCS mechanism achieves improvement on tumor and lesion being detected at an early stage compared to the state-of-the-art methods.

REFERENCES

- Duan, C., Z. Liang, S.L. Bao, H.B. Zhu, S. Wang, G.X. Zhang, J.J. Chen and H.B. Lu, 2010. A coupled level set framework for bladder wall segmentation with application to MR cystography. *IEEE T. Med. Imaging*, 29(3): 903-915. ieeexplore.ieee.org/xpls/abs_all.jsp?arnumber=5423297.
- Huang, H., A.B. Tosun, J. Guo, C. Chen, W. Wang, J.A. Ozolek and G.K. Rohde, 2014. Cancer diagnosis by nuclear morphometry using spatial information. *Pattern Recogn. Lett.*, 42(1): 115-121. <http://www.sciencedirect.com/science/article/pii/S016786551400049X>.
- Layer, T., M. Bläckner, B. Knäus, D. Georg, J. Neuwirth, R.P. Baum, C. Schuchardt, S. Wiessalla and G. Matz, 2015. PET image segmentation using a Gaussian mixture model and Markov random fields. *EJNMMI Phys.*, 2: 9. <http://www.ncbi.nlm.nih.gov/pmc/articles/PMC4545759/>.
- Liu, J., S. Wang, M.G. Linguraru, J. Yao and R.M. Summers, 2014. Tumor sensitive matching flow: A variational method to detecting and segmenting perihepatic and perisplenic ovarian cancer metastases on contrast enhanced abdominal CT. *Med. Image Anal.*, 18(5): 725-739. <http://www.ncbi.nlm.nih.gov/pubmed/24835180>.
- Liu, J., S. Wang, M.G. Linguraru, J. Yao and R.M. Summers, 2015. Computer-aided detection of exophytic renal lesions on non contrast CT images. *Med. Image Anal.*, 19(1): 15-29. <http://www.sciencedirect.com/science/article/pii/S1361841514001133>.
- Madooei, A., M.S. Drew, M. Sadeghi and M.S. Atkins, 2013. Automatic detection of blue-white veil by discrete colour matching in dermoscopy images. *Med. Image Comput. Comput. Assist. Interv.*, 16(pt 3): 453-460. <http://www.ncbi.nlm.nih.gov/pubmed/24505793>.
- Mendoza, C.S., N. Safdar, K. Okada, E. Myers, G.F. Rogers and M.G. Linguraru, 2014. Personalized assessment of craniosynostosis via statistical shape modeling. *Med. Image Anal.*, 18(4): 635-646. <http://www.ncbi.nlm.nih.gov/pubmed/24713202>.
- Sadeghi, M., T.K. Lee, D. McLean, H. Lui and M.S. Atkins, 2013. Detection and analysis of irregular streaks in dermoscopic images of skin lesions. *IEEE T. Med. Imaging*, 32(5): 849-861. <http://www.ncbi.nlm.nih.gov/pubmed/23335664>.
- Wang, L., F. Shi, G. Li, Y. Gao, W. Lin, J.H. Gilmore and D. Shen, 2014. Segmentation of neonatal brain MR images using patch-driven level sets. *Neuroimage*, 84: 141-158. <http://www.sciencedirect.com/science/article/pii/S1053811913008628>.
- Zhao, Q., K. Okada, K. Rosenbaum, L. Kehoe, D.J. Zand, R. Sze, M. Summar and M.G. Linguraru, 2014. Digital facial dysmorphology for genetic screening: Hierarchical constrained local model using ICA. *Med. Image Anal.*, 18(5): 699-710. <http://www.sciencedirect.com/science/article/pii/S1361841514000486>.